

Highly Oriented Self-Assembled Monolayers as Templates for Epitaxial Calcite Growth

A. Markus Travaille, Lotte Kaptijn, Paul Verwer, Bas Hulsken,
Johannes A. A. W. Elemans, Roeland J. M. Nolte, and Herman van Kempen*

Contribution from the NSRIM Institute, University of Nijmegen, Toernooiveld 1,
6525 ED Nijmegen, The Netherlands

Received February 12, 2003; E-mail: hvk@sci.kun.nl

Abstract: The lateral alignment of {012} habit-modified calcite crystals with respect to a carboxylic acid terminated self-assembled monolayer (SAM) of thiols has been determined. The crystals were grown from a Kitano solution (pH 5.6–6.0), and the samples were investigated with scanning electron microscopy, X-ray diffraction, and polarization microscopy. For the first time, a lattice match in one direction, which is the nearest neighbor direction of the SAM and the calcite <100> direction, has been experimentally shown. The experimental results are in good agreement with the theoretical models proposed in previous work, and it is expected that this method can be applied to similar systems where inorganic crystals nucleate with a preferred orientation to a SAM.

Introduction

One of the most striking features of crystalline materials formed in organisms is that they generally do not resemble their synthetic counterparts in morphology and physical properties.¹ Although these materials have the same basic structure, they can have a different shape and strength because the bioorganism controls their crystal morphology and the number of defects in a single crystal. This control is usually exerted by means of a matrix of bioorganic compounds which influence the nucleation and growth direction of the inorganic crystals.^{1,2} Calcium carbonate, and in particular calcite, is an important mineral in organisms because it is widely used by nature to give strength and shape to organisms.³

Previous work has shown that Langmuir monolayers^{4,5} and self-assembled monolayers (SAMs)^{6–10} can act as templates for the nucleation of calcite. Depending on the structure of the monolayer and the type of endgroup functionality, different calcite faces are nucleated.⁶ Most of these templates are very selective in nucleating a particular crystal face, but only in a few cases has a lateral alignment between the monolayer and the crystals been observed.^{11–13} Such an alignment can occur

only if the structure of the monolayer is homogeneous all over the substrate and if a unique interaction exists between the monolayer and the calcite face that is nucleated. In a previous paper, we have described a method to laterally align calcite crystals using a SAM of carboxylic acid functionalized thiols as a template.¹³ However, the number of crystals that could be grown with this method was too small to measure this lateral orientation by X-ray diffraction, and therefore the precise lateral orientation of the nucleated crystal face with respect to the SAM remains as yet uncertain. Here, we present a new procedure to grow a sufficient amount of calcite crystals on a SAM of functionalized thiols on Au(111), and this enabled us for the first time to determine the exact orientation between the Au(111) lattice and the nucleated calcite crystals. The fact that the calcite crystals were aligned with respect to the Au(111) lattice implies that the thiol monolayer is well defined and behaves like a 2D crystal and that the interaction between the carboxylic acid groups of the thiols and the calcite crystals is unique. So far, it has been impossible, however, to determine the exact geometry of the molecules and ions at the thiol–calcite interface, because only indirect information is available about the precise orientation of the carboxylic acid groups of the thiols. Although the models that are presented in this paper have some uncertainties, our data allow us to present a more precise model for the interaction between carboxylic acid functional groups and calcite crystals than was possible until now.

Results and Discussion

The SAMs were constructed by placing gold films, which were evaporated on a freshly cleaved mica substrate, into a 0.1

- (1) Berman, A.; Addadi, L.; Weiner, S. *Nature* **1988**, *331*, 546.
- (2) Berman, A.; Addadi, L.; Kvick, A.; Leiserowitz, I.; Nelson, M.; Weiner, S. *Science* **1990**, *250*, 664.
- (3) Lowenstam, H. A.; Weiner, S. *On Biomineralization*; Oxford University Press: New York, 1999.
- (4) Rajam, S.; Heywood, B. R.; Walker, J. B. A.; Mann, S. *J. Chem. Soc., Faraday Trans.* **1991**, *87*, 727.
- (5) Heywood, B. R.; Rajam, S.; Mann, S. *J. Chem. Soc., Faraday Trans.* **1991**, *87*, 735.
- (6) Aizenberg, J.; Black, A. J.; Whitesides, G. M. *J. Am. Chem. Soc.* **1999**, *121*, 4500.
- (7) Aizenberg, J.; Black, A. J.; Whitesides, G. M. *Nature* **1999**, *398*, 495.
- (8) Kuether, J.; Tremel, W. *Thin Solid Films* **1998**, *327–329*, 554.
- (9) Kuether, J.; Nelles, G.; Seshadri, R.; Schaub, M.; Butt, H.-J.; Tremel, W. *Chem.-Eur. J.* **1998**, *4*, 1834.
- (10) Kuether, J.; Seshadri, R.; Knoll, W.; Tremel, W. *J. Mater. Chem.* **1998**, *8*, 641.

- (11) Berman, A.; Ahn, D. J.; Lio, A.; Salmeron, M.; Reichert, A.; Charyc, D. *Science* **1995**, *269*, 515.
- (12) Yang, J.; Meldrum, F. C.; Fendler, J. H. *J. Phys. Chem.* **1995**, *99*, 5500.
- (13) Travaille, A. M.; Donners, J. J. M.; Gerritsen, J. W.; Sommerdijk, N. A. J. M.; Nolte, R. J. M.; van Kempen, H. *Adv. Mater.* **2002**, *14*, 492.

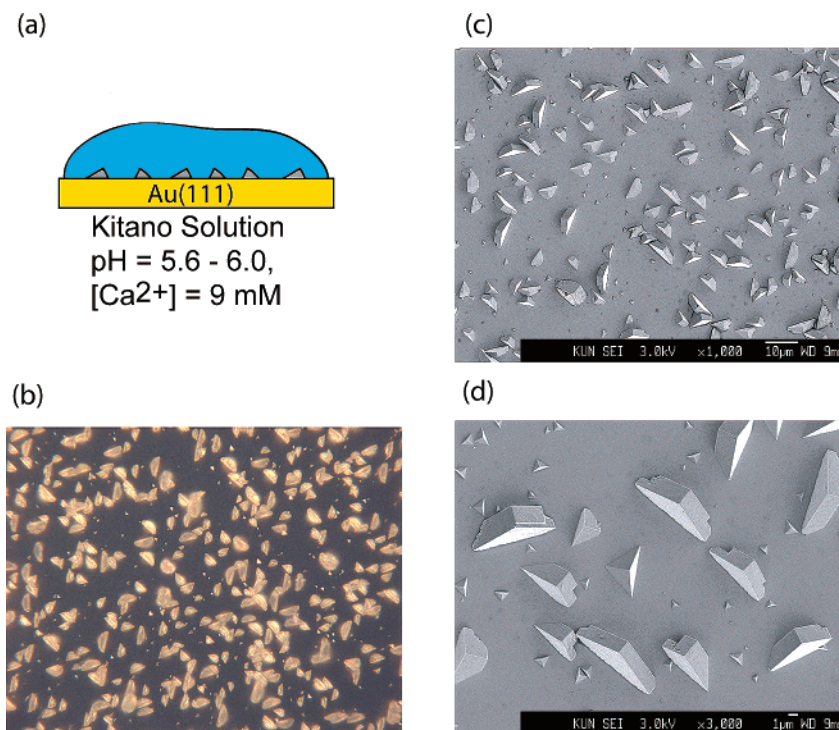
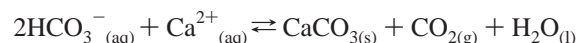


Figure 1. (a) Calcite growth from a droplet of a Kitano solution. (b) Polarization micrograph of growing calcite crystals (1000 \times). (c) Scanning electron micrograph of calcite grown on a self-assembled monolayer of MHA (1000 \times). (d) Scanning electron micrograph zoomed in on laterally aligned calcite crystals (3000 \times).

mmol solution of 16-mercaptohexadecanoic acid (MHA) in ethanol for 1 h at 55 $^{\circ}\text{C}$. The samples were subsequently rinsed with ethanol to remove the unbound thiols and with Nanopure water to remove the ethanol. A droplet of a Kitano solution¹⁴ was deposited onto the samples. The latter solution is based on the equilibrium:



The supersaturation of this solution depends on the degassing velocity of CO_2 , which causes the calcite growth to take place mainly at the air/water interface because at that point the CO_2 concentration is minimal and, therefore, the supersaturation is maximal. Previously, the sample was placed upside down in a vessel filled with this solution,¹³ but the number of nucleation events at the SAM was rather low. To increase the CO_2 degassing speed, and thus the supersaturation at the SAM, the sample was placed with the SAM facing upward, and when only a droplet of the Kitano solution was placed on the sample the distance between the SAM and the air/water interface was kept minimal (Figure 1a). The crystallization was followed in situ with a polarization microscope (Figure 1b). From Figure 1c and 1d, it can be seen that the number of nucleated crystals is very high. The total time needed for the crystals to nucleate and grow was approximately 1 h, which is relatively short, as compared to the time of 24 h needed for our previously reported method.¹³

The samples obtained were also studied with scanning electron microscopy (SEM) and X-ray diffraction. The SEM images (Figure 1c and 1d) revealed that the majority of the calcite crystals had a size ranging from 1 to 5 μm and that they were nucleated with the $\{012\}$ face parallel to the SAM. The observation that many of the crystals in Figure 1d have the same

orientation already suggests the existence of a lateral alignment between the crystals. The Miller indices of the nucleated faces can be determined by measuring the angles between three adjacent $\{104\}$ faces in a SEM image which has to be recorded in a direction perpendicular to the Au(111) film,^{6,15,16} and by measuring a $\theta/2\theta$ X-ray diffraction pattern in which the peak positions and heights of the calcite crystals are compared to those of an ideal calcite powder (Figure 2).^{6,17} During this $\theta/2\theta$ scan, the sample was rotated to average the intensity of the diffraction signal, so that the height of the peaks does not depend on the in-plane direction of the sample.

In the X-ray diffraction pattern that was recorded of the calcite crystals on the SAM, only peaks corresponding to the $\{012\}$ and $\{104\}$ faces were present. When the relative intensities of the $\{012\}$ and $\{104\}$ peaks are compared to those in the spectrum of an ideal calcite powder, it can be concluded that >95% of the crystals are oriented with their $\{012\}$ face parallel to the SAM. The pole plots in Figure 2c and 2d show that the interaction between the SAM and the calcite $\{012\}$ plane is unique because the width and shape of the Au(111) peak is the same as the width and shape of the calcite $\{012\}$ peak. The results are in agreement with the results obtained with SEM. The small $\{104\}$ peak in the diffraction pattern might originate from a few crystals that dropped from the solution onto the SAM. In some cases, these $\{104\}$ oriented crystals were also

(14) Kitano, Y. *Bull. Chem. Soc. Jpn.* **1962**, *35*, 1972.

(15) Archibald, D. D.; Qadri, S. B.; Gaber, P. B. *Langmuir* **1996**, *12*, 538.

(16) The precision of this method is about $\pm 1.5^{\circ}$ and therefore less accurate than results obtained with the XRD method. However, the SEM images clearly show that almost all of the crystals have an orientation that fits with the $\{012\}$ orientation. Only a few crystals were observed that had the $\{104\}$ plane parallel to the SAM.

(17) Joint Committee on Powder Diffraction Standards International Center for Diffraction Data, Swarthmore, U.K., 1986; File No. 5-586.

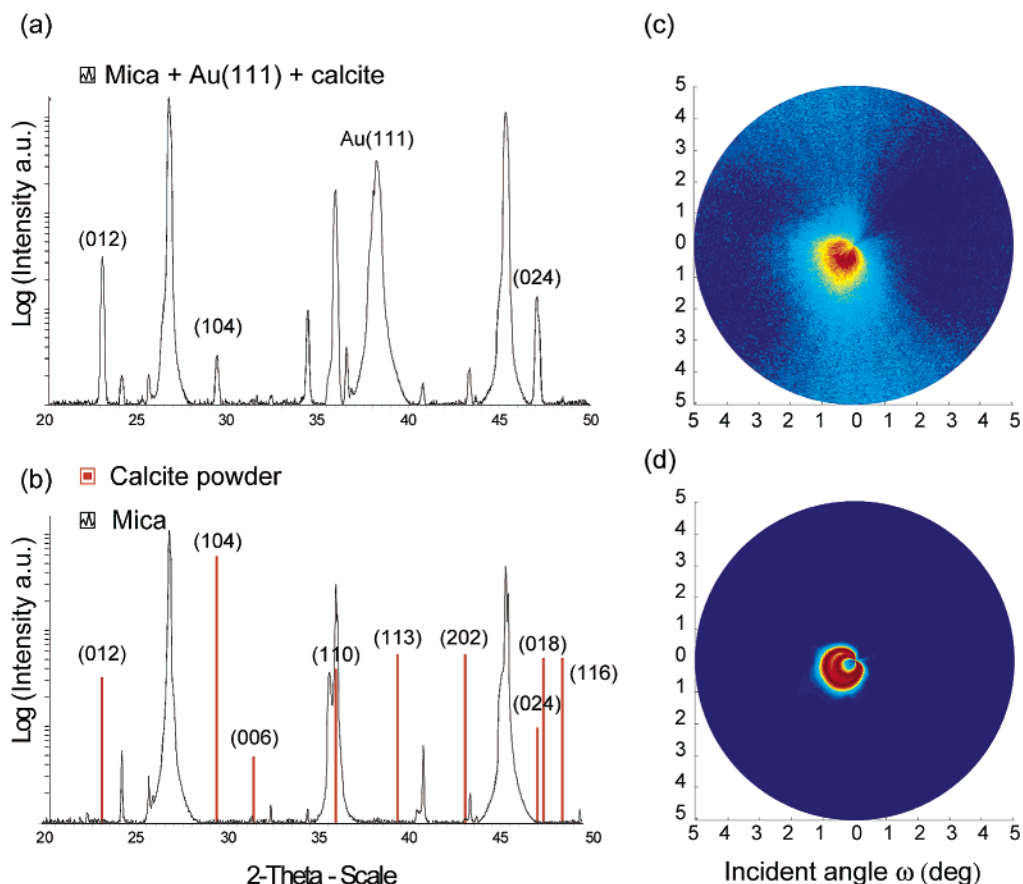


Figure 2. (a) X-ray diffraction patterns of mica + Au(111) + oriented calcite (the samples were rotated around the surface normal axis during the measurements). The indices in the spectrum represent the calcite crystal planes that are parallel to the SAM. (b) X-ray diffraction patterns of mica and calcite powder. The red lines represent the peak heights and positions of an ideal calcite powder (diffraction indices for calcite are given in the spectrum), and the peaks belonging to the mica were obtained by measuring a blanco mica sample. (c) Polar plot of the calcite {012} peak. (d) Polar plot of the Au(111) peak. The shape of both peaks in Figure 2c and 2d is a little bit distorted due to a misalignment of the azimuthal axis and the Au[111] and calcite {012} directions.

observed with SEM and polarization microscopy (data not shown).

Previous experiments had demonstrated that the nucleated calcite face was the {012} face (a model is shown in Figure 3a) and that the crystals are laterally oriented with respect to each other as well as to the SAM.¹³ This implies that there exists a unique interaction between the carboxylic acid groups of the SAM and the nucleated calcite crystals. The geometry of this interaction can be determined with X-rays when the in-plane orientation of the SAM and the calcite crystals is measured simultaneously.¹⁸ We have chosen to measure the in-plane orientation of the Au(111) lattice with respect to the in-plane orientation of the calcite {012} crystals and relate the structure and orientation of the SAM to the orientation of the Au(111) lattice. In principle, this can be easily done by measuring a pole figure of the sample. The in-plane orientations from Au(111) and calcite {012} would follow directly from such a measurement. There are, however, some practical problems when this technique is applied without any further considerations. The number of calcite crystals is rather small, and for each orientation only one-sixth of the signal generated from the calcite crystals will be measured, if we assume that each orientation is equally present in our sample. The fact that the {012} planes of the calcite crystals are parallel to the Au(111) film can be

used to select only one calcite plane and one gold plane which will provide the in-plane orientations. In this way, the time needed to obtain the results is drastically reduced, but still a measurement time of 20 h was needed to obtain a sufficient signal-to-noise ratio. One of the reasons why the measurement time is so long is that, due to the sample geometry and the diffractometer setup, it was very difficult to align the azimuthal axis (φ) with the Au[111] direction. Therefore, it was necessary to measure the spectra for different incident angles around a theoretical value to obtain the positions of all of the calcite and gold peaks.

The sample, mounted on a goniometer (setup in Figure 3b), was rotated about the azimuthal axis with the beam and detector put in the diffraction setup for calcite {122} and Au{113} planes, respectively. This ensures that, upon rotation of the sample, distinct peaks will appear if the crystals are laterally oriented and a uniform signal will appear if they are not oriented. Because the Au{113} planes have a six-fold symmetry around the Au[111] axis, six peaks can be expected for the gold film. The azimuthal angle corresponding to a peak indicates directly the nearest neighbor (NN) direction of the Au(111) film. The calcite {122} planes, however, have besides the six different orientations of the crystals an extra symmetry element, the mirror plane of the {012} face indicated by the yellow line in Figure 3a. Each orientation of a calcite crystal will therefore give rise to two azimuthal angles for which diffraction will

(18) This, however, would require measurements at a synchrotron facility because the diffracted signal from the SAM is very weak.

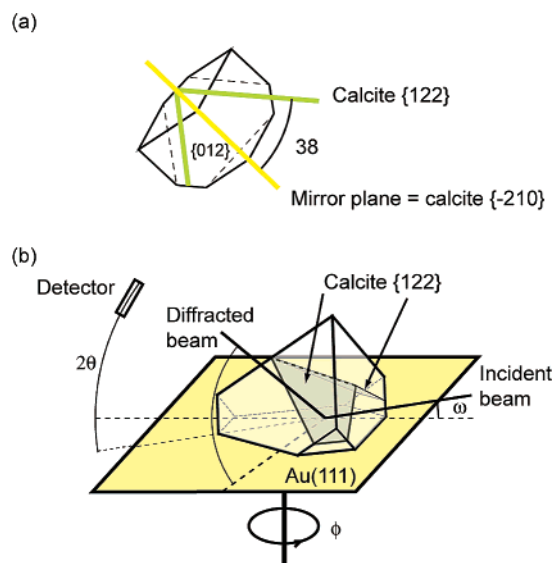


Figure 3. (a) Model of a $\{012\}$ oriented calcite crystal. The yellow line, which represents the mirror plane, which is the $\{-210\}$ calcite plane and is perpendicular to the $\{012\}$ face and parallel to the $[001]$ axis, determines the lateral orientation of the crystal. The green lines represent the lateral orientations of the $\{122\}$ planes. (b) Schematic model of the diffraction setup. The angle between the incident beam and the detector (2θ) is such that only diffraction from the calcite $\{122\}$ planes will be detected. When the sample is rotated about ϕ , diffraction will occur every time the calcite $\{122\}$ plane is correctly aligned with respect to the incoming beam and the detector. The incident angle ($\omega = \theta - \alpha$) is varied around the equilibrium value to correct for the misalignment between the Au $[111]$ axis and ϕ , where α is the angle between the Au (111) plane and the selected calcite $\{122\}$ plane.

occur. These azimuthal angles are deviated $+38^\circ$ and -38° from the mirror plane, and the theoretical spectrum for diffraction on the calcite $\{122\}$ planes is drawn as an inset in Figure 4a.

The calcite $\{122\}$ and Au $\{113\}$ planes were selected by two criteria: the relative intensities of the peaks, obtained from the powder diffraction data, should be maximal, and the diffraction angle should fit in the geometry of our diffraction setup ($\omega = (\theta - \alpha) > 0$ and thus $\theta > \alpha$, where α is the angle between the Au (111) plane and the selected calcite and gold planes).

The measured spectrum of the calcite crystals is shown in Figure 4a, and the spectrum for the gold surface is shown in Figure 4b. From the theoretical spectra, 12 peaks are expected for calcite (peak positions indicated by black dots in Figure 4a) and 6 peaks for gold. However, from Figure 4b it is clear that 12 gold peaks are measured (white spots in Figure 4b). Six peaks have a high intensity and six peaks have a lower intensity and are shifted by 30° . A possible explanation for this might be that the Au (111) islands follow the symmetry of the underlying mica but that in some parts of the sample the orientation of the islands is rotated 30° due to a mismatch between the Au (111) and the mica lattice.

From Figure 4a and 4b, it can be concluded that the azimuthal axis is not aligned parallel to the Au $[111]$ axis, which causes a precession of the Au $[111]$ axis around the rotation axis, and this in turn causes a sine-shaped distribution of the peak positions around an equilibrium value of ω .

From the data in Figure 4, the orientation of the calcite crystals with respect to the Au (111) film can be directly derived. The azimuthal widths of the peaks in the spectra for Au and calcite are the same, and this indicates that the in-plane orientation of the calcite crystals is uniquely defined by the in-

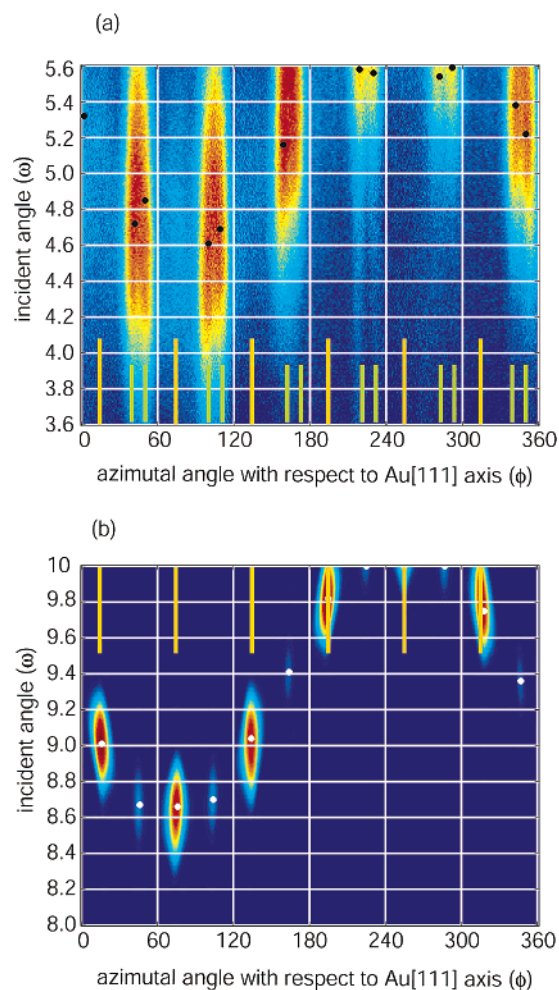


Figure 4. (a) X-ray diffraction pattern of the calcite $\{122\}$ planes. The black spots indicate the peak positions; the yellow lines correspond to the section between the $\{012\}$ face and the $\{-210\}$ mirror plane, and they represent the lateral orientations of the calcite crystals; and the green lines represent the calculated positions of the calcite $\{122\}$ peaks. (b) X-ray diffraction pattern of the Au $\{113\}$ planes. The peak positions (white spots) directly indicate the nearest neighbor direction. The yellow lines represent the orientation of the calcite crystals.

plane orientation of the Au (111) film. With these data, and the known parameters for the orientation of the molecules in the SAM with respect to an Au (111) film,¹⁹ a model can be constructed in which only the positions of the different ions and molecules are taken into account (Figure 5). It is well known that thiol monolayers form a highly organized, densely packed monolayer on Au (111) substrates. For these monolayers, two structures have been proposed in the literature, one in which the thiols are arranged in a $R30^\circ(\sqrt{3} \times \sqrt{3})$ and one in which they are arranged in a $C2 \times 4$ lattice on the Au (111) plane.¹⁹ Although the models differ in the orientation of the alkane backbones (vide infra), the positions of the carboxylic acid endgroups are the same in both cases. For reasons that will be discussed below, only the carbonate ions of the calcite $\{012\}$ face are shown. It can be easily seen that a lattice match exists between the SAM and the calcite $\{012\}$ face in the a -direction (calcite $\langle 100 \rangle$), but not in the b -direction (calcite $\langle 12-1 \rangle$). Such an orientation has already been tentatively proposed by Aizenberg et al.⁶ The b -direction corresponds to the section between

(19) Schreiber, F. *Prog. Surf. Sci.* **2000**, *65*, 151.

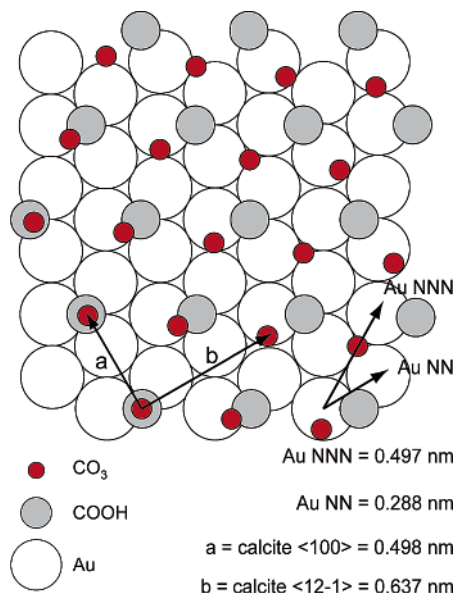


Figure 5. Schematic drawing of the lattices of the Au(111) plane, the carboxylic acid endgroups of the SAM, and the carbonate ions of the calcite lattice. The lattice match in the a -direction is almost perfect, but there is a large mismatch in the b -direction. All three lattices can be translated in any direction; therefore, their precise positions remain unclear.

the {012} face and the $\{-210\}$ mirror plane, and its direction is represented by the yellow lines in Figure 4. This direction is parallel to the NN direction of the Au(111) plane.

The lattice match in one direction might explain the fact that the calcite crystals have a unique orientation with respect to the SAM; however, it does not explain why the {012} face is selectively nucleated. Intuitively, one would expect nucleation of the calcite {001} face because the Ca^{2+} ions in this plane have a hexagonal lattice that perfectly matches the hexagonal lattice of the SAM. Another question is whether at the interface the calcite crystal is Ca^{2+} or carbonate terminated. Because it can be expected that the MHA monolayer is completely protonated at the starting pH²⁰ of the Kitano solution (pH = 5.5–6.0), which is lower than the reported $\text{p}K_a$ value of 6.5 of a SAM of MHA on Au(111) films,²¹ there will be no strong electrostatic preference for one of these ions. Although the {012} face does not have a perfect lattice match with the SAM, the interaction between the SAM and the calcite crystals must have a preferred direction, because the orientation of the crystals is highly defined. It is therefore proposed that the carbonate ions are nucleated first and that the directionality and the selectivity for the {012} face is caused by the orientation of the carboxylic acid endgroups and by the presence of hydrogen bridges between the carboxylic acid endgroups and the carbonate ions. Aizenberg et al. have claimed that the Ca^{2+} ions are deposited first,⁶ but their results have been obtained from a crystallization solution with a starting pH²⁰ of 7.0–7.5 which is well above the reported $\text{p}K_a$ value of a SAM of MHA. Therefore, the SAM they used was negatively charged, which causes a strong electrostatic attraction with the Ca^{2+} ions.

(20) The starting pH of a crystallization solution is defined as the pH of the solution at the moment the samples are placed in the solution. The pH at which the crystallization starts is as yet unknown, but we assume that it depends on the pH value of the starting solution. Experiments regarding this issue are currently in progress and will be reported elsewhere.

(21) Lee, T. R.; Carey, R. I.; Biebuyck, H. A.; Whitesides, G. M. *Langmuir* **1994**, *10*, 741.

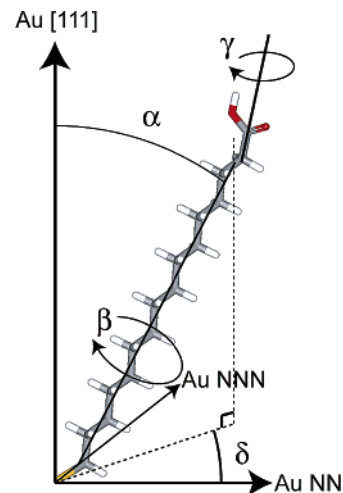


Figure 6. 16-Mercaptohexadecanoic acid (MHA) and its degrees of freedom. In our models, the tilt angle α is 32° and the tilt direction δ is 22.7° . The twist angle for the $R30^\circ(\sqrt{3} \times \sqrt{3})$ model is $\beta = 55^\circ$ and for the $C2 \times 4$ model is $\beta = +35^\circ$ and -55° . The carboxylic acid endgroup is free to rotate around γ .

To get a better idea about the precise interactions between the carboxylic acid endgroups of the SAM and the calcite crystal, 3D models were constructed which take into account all known parameters of a SAM of thiols on Au(111).¹⁹ Although the information available about the orientation of the carboxylic acid groups of the thiols is only limited, it is still of general interest to create such a model because it illustrates the complexity of the problem of nucleation behavior of calcite on organic substrates. For the construction of the 3D models (Figure 7), which were generated using the Cerius2 software package,²² the two models have been used which have been mentioned before for the structure of the SAM of alkanethiols on Au(111) surfaces.¹⁹ In both models, the alkane backbones and the carboxylic acid endgroups have the same positions, but in the model with the $C2 \times 4$ lattice the orthogonal orientation and the pairing of the sulfur atoms break the hexagonal symmetry of the monolayer and give rise to the orthorhombic unit cell. The sulfur atoms of the chains with a different twist angle are paired, and as a result gauche defects are present in the alkane chains.²³ This sulfur pairing causes a height modulation of the carboxylic acid endgroups, and, due to the fact that the alkane chains are orthogonal with respect to each other, these endgroups adopt different orientations. The other parameters, such as the tilt angle α , and the twist angle of the alkane chains β , and the tilt direction δ , are well established for alkanethiols¹⁹ (see Figure 6).

However, most structural data for thiol monolayers have been obtained for methyl terminated thiols, and only a few studies have been carried out on carboxylic acid terminated thiols.^{24–26} Some of those studies have shown that the thiols are ordered in a hexagonal $R30^\circ(\sqrt{3} \times \sqrt{3})$ lattice, but with a smaller coherence length than in the case of methyl terminated thiols, although the presence of a solution containing Ca^{2+} or Mg^{2+} ions was found to improve the ordering.²⁵ Recent scanning

(22) Cerius2 User Guide, March 1997, Accelrys Inc., 9685 Scranton Road, San Diego, CA 92121-3752.

(23) Fenter, P.; Eberhardt, A.; Eisenberger, P. *Science* **1994**, *266*, 1216.

(24) Dannenberger, O.; Weiss, K.; Himmel, H.-J.; Jäger, B.; Buck, M.; Wöll, Ch. *Thin Solid Films* **1997**, *307*, 183.

(25) Li, J.; Liang, K. S.; Scoles, G.; Ulman, A. *Langmuir* **1995**, *11*, 4418.

(26) Li, L.; Chen, S.; Jiang, S. *Langmuir* **2003**, *19*, 3266.

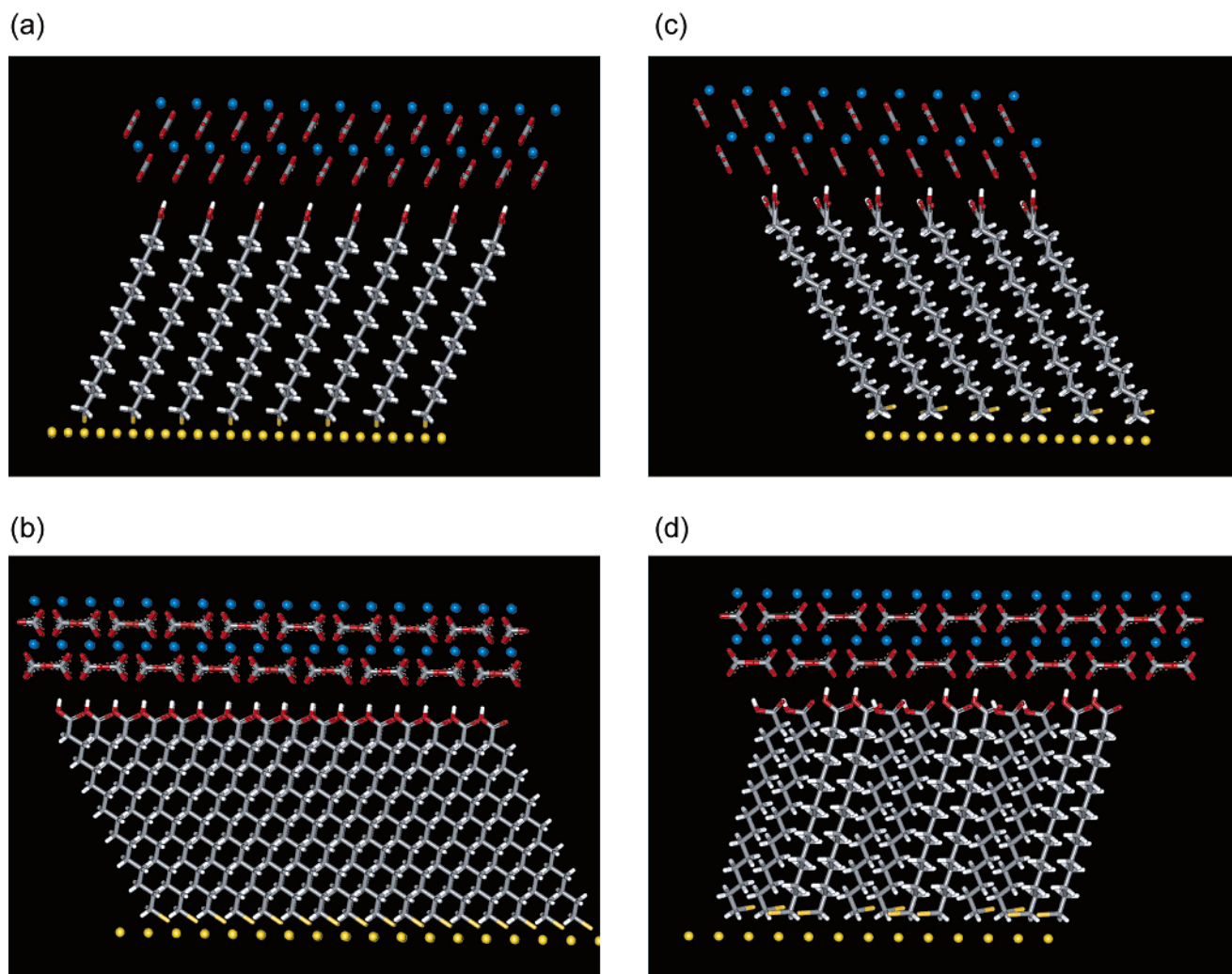


Figure 7. 3D models of calcite crystals nucleated with their {012} faces on a SAM of MHA on Au(111). (a) $R30^\circ(\sqrt{3} \times \sqrt{3})$ structure viewed in the a -direction of Figure 5. Note the directional match between the carboxylic acid endgroups and the carbonate ions. (b) $R30^\circ(\sqrt{3} \times \sqrt{3})$ structure viewed in the b -direction of Figure 5. In this direction, a lattice match exists between the SAM and the carbonate ions. (c) $C2 \times 4$ structure viewed in the a -direction of Figure 5. Note the directional match between one-half of the carboxylic acid endgroups and the carbonate ions. (d) $C2 \times 4$ structure viewed in the b -direction of Figure 5. In this direction, a lattice match exists between the SAM and the carbonate ions, although it is obvious that in this model the interaction is less directional.

tunneling microscopy studies have revealed that carboxylic acid terminated thiol monolayers, when prepared at elevated temperatures, form larger domains with a hexagonal $R30^\circ(\sqrt{3} \times \sqrt{3})$ lattice than when prepared at room temperature.²⁶ Because our experiments have demonstrated that the calcite crystals are oriented over very large distances, we propose that the SAM of MHA has a similar structure as a SAM of methyl terminated thiols, whether that would be the $R30^\circ(\sqrt{3} \times \sqrt{3})$ structure or the $C2 \times 4$ structure, but in both structures the carboxylic acid groups are free to rotate around the angle γ and this results in a disordered structure of the endgroups.^{19,24}

In our models (Figure 7), we have optimized the angle γ in such a way that there is a hydrogen-bonding interaction between the carboxylic acid endgroups and the carbonate ions and, in addition, that the endgroups and the carbonate ions are oriented in the most parallel geometry. It is obvious that the model in which the thiols are arranged with the $R30^\circ(\sqrt{3} \times \sqrt{3})$ applies the best to these two criteria, although as yet we have no conclusive experimental evidence for one of the two models.

Conclusion

In this paper, we have presented a new method to grow a high density of calcite crystals with a preferred {012} nucleation face on a SAM of carboxylic acid terminated thiols. This high density of crystals allowed us to identify the precise orientation of the calcite crystals with respect to the Au(111) lattice with X-ray diffraction techniques. The measurements showed that the crystals have six different in-plane orientations corresponding to the six-fold symmetry of the Au(111) surface which is translated by the SAM. These results show that there exists a unique interaction between the organic molecules of the SAM and the calcite crystals. By using the known parameters of a SAM on a Au(111) lattice, we found that there exists a lattice match between the NN direction of the SAM and the calcite $\langle 100 \rangle$ direction in the calcite {012} plane. Such a lattice match in one direction has also been suggested by Aizenberg et al. in their model for calcite {015} oriented nucleation. The difference in orientation of the calcite crystals with the results of Aizenberg et al. might be explained by the fact that they used a different

crystallization solution with a different starting pH, which is above the pK_a value of a SAM of MHA, while the starting pH of the crystallization method applied in this work is below this value.

We have shown that by using this new method a verification of a general model for biomineralization is possible. The method also allows the study of other, related systems, where thiols with different functional groups, different chain lengths, and crystallization conditions with a different starting pH will be used. These investigations might lead to more detailed insight

into the physical and chemical nature of the interactions between the SAM and the calcite crystals.

Acknowledgment. Part of this work was supported by the Stichting voor Fundamenteel Onderzoek der Materie (FOM), which is financially supported by the Stichting voor Nederlands Wetenschappelijk Onderzoek (NWO). We thank J. Gerritsen, Dr. H. Meekes, Dr. J deYoreo, Dr. C. Orme, Dr. R. de Gelder, and Prof. E. Vlieg for fruitful discussions.

JA034624R